THE JOURNAL OF PHYSICAL CHEMISTRY A

Article

pubs.acs.org/JPCA

Branching Ratio Measurements for Vacuum Ultraviolet Photodissociation of $^{12}C^{16}O$

Hong Gao,[†] Yu Song,[†] Yih-Chung Chang,[†] Xiaoyu Shi,[†,‡] Qing-Zhu Yin,[‡] Roger C. Wiens,[§] William M. Jackson,*[,†] and C. Y. Ng*[,†]

[†]Department of Chemistry, University of California, Davis, California 95616, United States

[‡]Department of Geology, University of California, Davis, California 95616, United States

[§]Los Alamos National Laboratory, Los Alamos, New Mexico 87545, United States

ABSTRACT: The branching ratios for the spin-forbidden photodissociation channels of $^{12}C^{16}O$ in the vacuum ultraviolet (VUV) photon energy region from 102 500 (12.709 eV) to 106 300 cm^{-1} (13.180 eV) have been investigated using the VUV laser time-slice velocity-map imaging photoion technique. The excitations to three $^1\Sigma^+$ and six $^1\Pi$ Rydberg-type states, including the progression of W(3sσ) $^1\Pi(v' = 0, 1,$ and 2) vibrational levels of CO, have been identified and investigated. The branching ratios for the product channels $C(^3P) + O(^3P)$, $C(^1D) + O(^3P)$, and $C(^3P) + O(^1D)$ of these predissociative states are found to depend on the electronic, vibrational, and rotational states of CO being excited. Rotation and e/f-symmetry dependences of the branching ratios into the spin-forbidden channels have been confirmed for several of the $^1\Pi$ states, which can be explained using the heterogeneous interaction with the repulsive $D'^1\Sigma^+$ state. The percentage of the photodissociation into the spin-forbidden channels is found to increase with increasing the rotational quantum number for the K(4pσ) $^1\Sigma^+$ ($v' = 0$) state. This has been rationalized using a $^1\Sigma^+$ to $^1\Pi$ to $^3\Pi$ coupling scheme, where the final $^3\Pi$ state is a repulsive valence state correlating to the spin-forbidden channel.

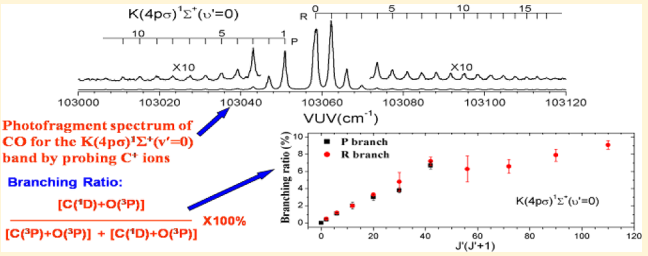

I. INTRODUCTION

Carbon monoxide (CO) photodissociation has drawn great attention over the past few decades because of its relevant application in the field of astrophysics.[1,2] Furthermore, as a simple diatomic molecule, the detailed photodissociation dynamics studies of CO have also made it a benchmark system for the comparison between state-of-the-art experimental measurements and theoretical predictions.[3,4] Most of the previous experimental work on CO is based on photoabsorption[5,6] and photoionization[7,8] measurements that involve the determination of photoabsorption cross-sections and predissociation line widths. Rotationally resolved predissociation rates and possible predissociation mechanisms have been deduced from these measurements. However, all the predissociation rates deduced from rotational line width measurements or pump−probe time-delay lifetime measurements[9] suffer from the inability to distinguish between the lowest three photodissociation channels, $C(^3P) + O(^3P)$, $C(^1D) + O(^3P)$, and $C(^3P) + O(^1D)$, when they are energetically available. The branching ratios for these dissociation channels allow the determination of the partial predissociation rates into these individual channels, which provide valuable information on the couplings between the directly photoexcited Rydberg states and the valence states correlating to the different predissociation product channels. Thus, the measurement of photofragment branching ratios or partial predissociation rates would open another platform for the investigation of predissociation dynamics other than the rotational line width and predissociation lifetime measurements, both of which can only provide the total predissociation rates. Okazaki and co-workers have collected photofragment spectra for the CO molecules by probing $C(^3P)$, $C(^1D)$, and $O(^3P)$.[10,11] They performed a detailed analysis on the photofragment spectra and compared the results with the simulated absorption spectra for the two Rydberg states L(4pπ) $^1\Pi(v' = 0)$ and L′(3dπ) $^1\Pi(v' = 1)$. The rotation and e/f-symmetry dependences of the branching ratios were observed for the L(4pπ) $^1\Pi(v' = 0)$ state, but not for the L′(3dπ) $^1\Pi(v' = 1)$ state. However, Okazaki et al. did not obtain any quantitative data for the branching ratios; and their detection sensitivity was insufficient for probing $C(^1D)$ atoms produced from other Rydberg states. Bakker et al.[12] used the combination of a tunable ArF excimer laser and the velocity-map imaging (VMI) technique to study the photodissociation channel $C(^1D) + O(^3P)$, but no branching ratio data could be deduced.

We have recently developed an experimental method to study the photodissociation dynamics of small molecules, which combines the tunable vacuum ultraviolet (VUV) laser radiation

Special Issue: Prof. John C. Wright Festschrift

Received: January 13, 2013
Revised: March 19, 2013

   dx.doi.org/10.1021/jp400412n | J. Phys. Chem. A XXXX, XXX, XXX−XXX

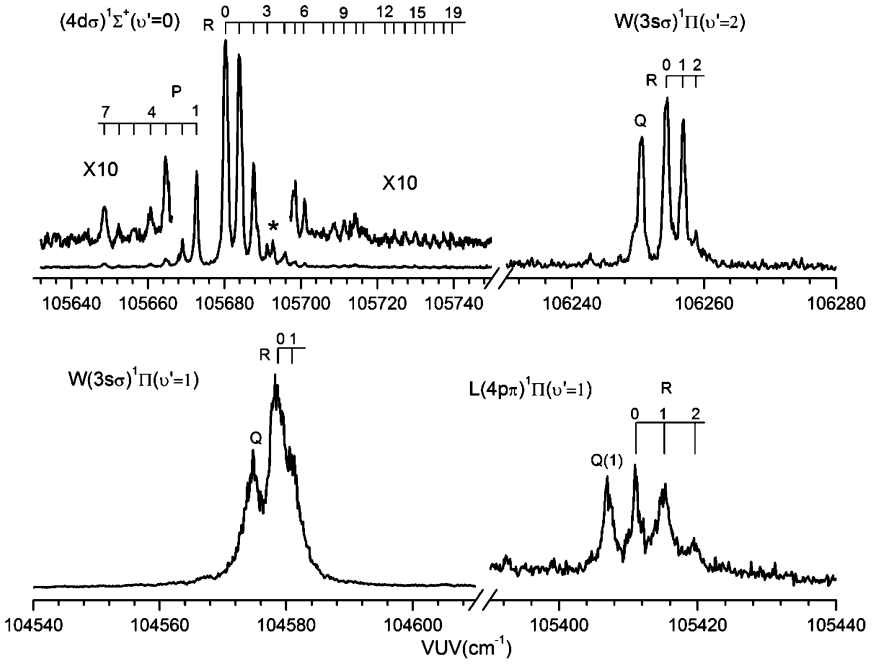

Figure 1. Carbon ion photofragment spectrum from 104 540 to 106 280 cm^{-1} (12.961−13.177 eV), covering the CO vibronic states W(3sσ) $^1\Pi(v' = 2)$, (4dσ) $^1\Sigma^+(v' = 0)$, L(4pπ) $^1\Pi(v' = 1)$, and W(3sσ) $^1\Pi(v' = 1)$. The relative intensities of these states were not normalized to the corresponding VUV intensities. With the exception of the C^+ ion photofragment spectrum for the L(4pπ) $^1\Pi(v' = 1)$ state, which was obtained by using the two independently tunable VUV lasers, all the spectra were obtained using a single VUV laser.

generated by two-photon resonance-enhanced four-wave mixing and the time-slice VMI-photoion (VMI-PI) method.[13,14] The product branching ratios in the predissociation of CO have been recently measured for the first time using this method in the energy region from 108 000 (13.390 eV) to 110 500 cm^{-1} (13.700 eV)[15,16] and were found to be strongly dependent on the vibronic states of CO that are excited. In the present study, we are extending these previous branching ratio measurements to the lower energy range from 102 500 (12.709 eV) to 106 300 cm^{-1} (13.180 eV). One important motivation of the present study is to provide quantitative branching ratio data and thus partial predissociation rate information on CO in the low energy region where accurate ab initio calculations are available. The branching ratio data obtained in this article are expected to be useful to benchmark theoretical calculations and establish accurate adiabatic potential energy curves that are needed to understand the predissociation dynamics of the CO molecule. Compared with the isoelectronic molecule N_2, the potential energy curves of CO are more complicated due to the lack of g/u symmetry, and as a result, its predissociation dynamics is still not well-known, especially the part that involves the homogeneous Π−Π interaction.[3,17] The matrix elements of a homogeneous interaction ($\Delta\Omega = 0$) are independent of the rotational quantum number J; while that of a heterogeneous interaction ($\Delta\Omega = \pm 1$) are proportional to $[J(J + 1) - \Omega_>]^{1/2}$, where $\Omega_>$ is the larger of the two Ω-values. Most of the previous investigations focused on the photodissociation dynamics of the ground product channel $C(^3P) + O(^3P)$ that produces ground state atoms so that there is very little information available about the spin-forbidden channels $C(^1D) + O(^3P)$ and $C(^3P) + O(^1D)$ that produce excited atoms. The present study rectifies this by providing information about all of the energetically allowed channels.

II. EXPERIMENTAL SECTION

The experimental methods used in the present study are the same as those described in the previous work,[16,18] and thus, they will only be briefly summarized here. A pulsed molecular beam of pure CO is produced by supersonic expansion through an Even−Lavie pulsed valve (EL-5-2004) with a nozzle diameter of 0.2 mm operating at 50 psi and 30 Hz. The molecular beam passes through two conical skimmers prior to entering the photodissociation/photoionization (PD/PI) region, where it is perpendicularly intersected by the VUV laser beam. The nascent C atoms thus produced from the photodissociation of CO are photoionized by the same VUV laser beam. The resulting C^+ ions are extracted and focused by the VMI ion optics onto a microchannel plate (MCP) detector. The electrons ejected from the MCP detector by ion impact are accelerated onto a phosphor screen to form an image that is recorded by a CCD camera.

The tunable VUV laser radiation generation system has also been described.[19] In the current study, we used Xe in the form of a gas jet as the nonlinear four-wave mixing medium. The UV wavelength is fixed at 222.568 nm (ω_1) that is resonant with the two-photon transition of Xe: $(5p)^5(^2P_{1/2})6p\ ^2[1/2](J = 0) \leftarrow (5p)^6\ ^1S_0$ at 89 860.015 cm^{-1}. The visible laser wavelength (ω_2) is scanned from 600 to 800 nm so that the sum-frequency ($2\omega_1 + \omega_2$) VUV laser has a range of 102 300−106 500 cm^{-1} (12.684−13.204 eV). In this experiment, the CO molecule is excited to each of the rovibronic states by the absorption of a sum-frequency VUV photon ($2\omega_1 + \omega_2$) and undergoes predissociation to produce carbon atoms in the ^3P and ^1D states. The carbon atoms thus produced are photoionized by absorbing another VUV photon ($2\omega_1 + \omega_2$) within the same VUV laser pulse, which is set at an energy above the ionization threshold of carbon atoms at 90 883.84 cm^{-1} (11.2682 eV).

We have two different experimental modes. In the first mode, we measure the rotationally resolved C^+ ion photofragment

dx.doi.org/10.1021/jp400412n | J. Phys. Chem. A XXXX, XXX, XXX−XXX

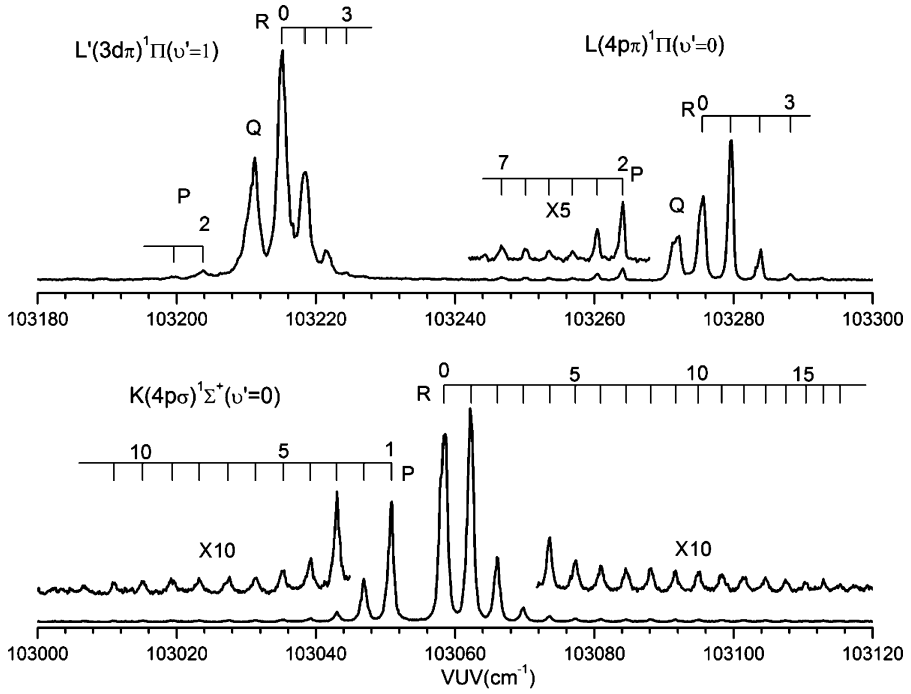

Figure 2. Carbon ion photofragment spectrum from 103 000 to 103 300 cm^{-1}, covering the CO vibronic states L(4pπ) $^1\Pi(v' = 0)$, L′(3dπ) $^1\Sigma^+(v' = 0)$, and K(4pσ) $^1\Sigma^+(v' = 0)$. The relative intensities of these states were not normalized to the corresponding VUV intensities.

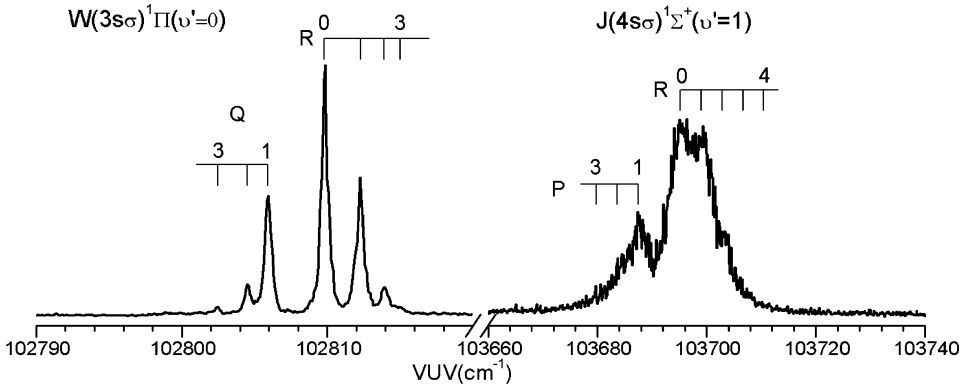

Figure 3. Carbon ion photofragment spectrum for the CO vibronic states J(4sσ) $^1\Sigma^+(v' = 1)$ and W(3sσ) $^1\Pi(v' = 0)$. The relative intensities of these states were not normalized to the corresponding VUV intensities.

spectra by gating on the C^+ ion peak in the time-of-flight (TOF) mass spectrum using a Boxcar data acquisition system (Stanford Research System, SR250) and scanning the VUV energy from 102 300 to 106 500 cm^{-1} (12.684−13.204 eV). The C^+ ion photofragment spectra confirm the previous photoabsorption and photoionization studies and are used to identify the frequencies of the rovibronic states of CO that are being investigated.

The second mode is concerned with time-sliced VMI-PI measurements. In this experiment, the VUV photon energy is fixed at a particular (E', v', J') state of CO, and the time-slice VMI-PI image is collected by applying a 40 ns high voltage pulse to the front MCP when C^+ ions arrive. The C^+ ions produced from different dissociation channels can be distinguished in the VMI images by their kinetic energies, and thus, the branching ratios of different photodissociation channels can be deduced from the total number of ions in an image at a particular kinetic energy. The analyses of the images that are collected provide the total kinetic energy release (TKER) spectra that are used to obtain the branching ratios.

III. RESULTS

The C^+ ion photofragment spectra obtained in the present study are shown in Figures 1−3. With the exception of the C^+ ion photofragment spectrum for the L(4pπ)$^1\Pi(v' = 1)$ state shown in Figure 1, which was obtained by using the two independently tunable VUV lasers (see the description given below), all the spectra of Figures 1−3 were obtained using a single VUV laser as described above. From the C^+ ion photofragment spectra shown in the figures, nine CO vibronic states between 102 700 and 106 300 cm^{-1} (12.733−13.180 eV) can be identified using the information from Table 1 of ref 2. The only state that was not observed is the H(4pσ) $^1\Sigma^+(v' = 1)$ level. This is probably due to the weak intensity of the VUV photolysis laser in the region of this band.

In time-slice VMI-PI measurements, the wavelength of the VUV laser is tuned to one of the rovibronic peaks indentified in

dx.doi.org/10.1021/jp400412n | J. Phys. Chem. A XXXX, XXX, XXX−XXX

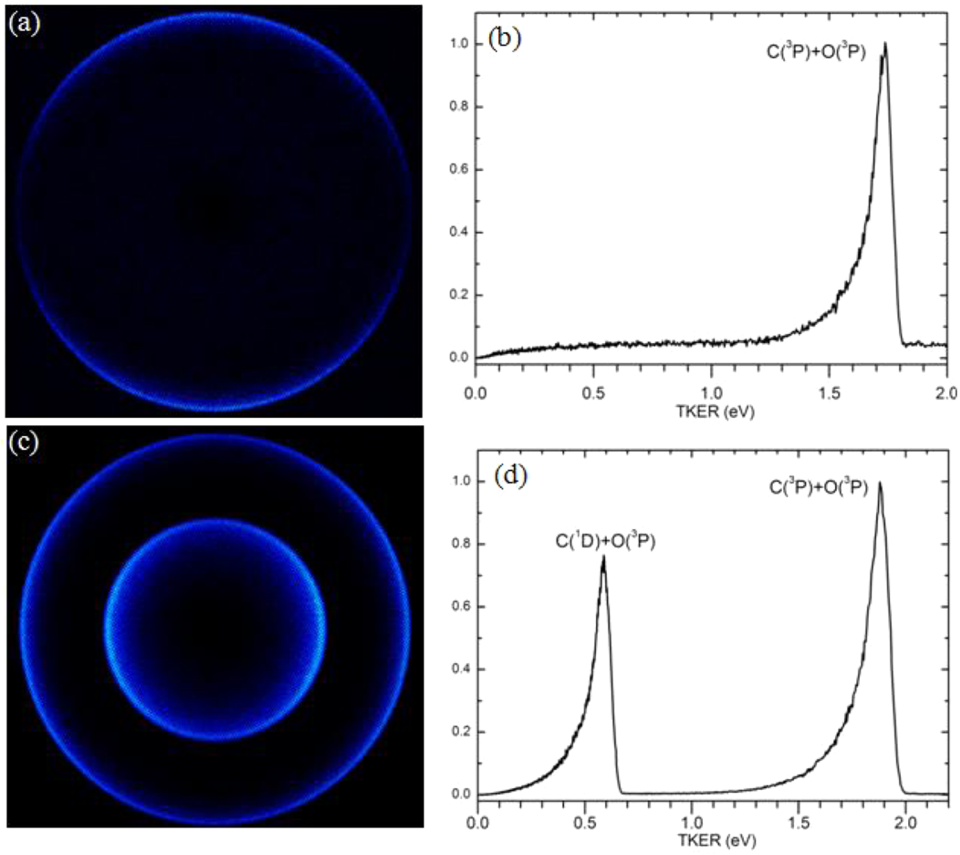

Figure 4. Time-slice VMI-PI images of C^+ ions and their TKER spectra produced from the predissociation of CO following the absorption of a single sum-frequency VUV photon at the R(0) lines of the state J(4sσ) $^1\Sigma^+(v' = 1)$ (a,b) at 103 695.8 cm^{-1} and the state W(3sσ) $^1\Pi(v' = 1)$ (c,d) at 104 578.7 cm^{-1}. The TKER spectra were normalized by treating the height of the $C(^3P) + O(^3P)$ peak as 1. The assignments for each of the peaks are shown in oanels b and d.

the C^+ ion photofragment spectra to collect the time-slice VMI-PI image of the C^+ ions, which are produced by VUV photoionization of the carbon atoms generated by VUV photodissociation of CO. Two of the typical time-slice VMI-PI images and their corresponding TKER spectra for the R(0) lines of the W(3sσ) $^1\Pi(v' = 1)$ level at 104 578.7 cm^{-1} and the J(4sσ) $^1\Sigma^+(v' = 1)$ level at 103 695.8 cm^{-1} are shown in Figure 4. On the basis of the TKER spectra, the W(3sσ) $^1\Pi(v' = 1)$ state dissociates into the $C(^1D) + O(^3P)$ spin-forbidden channel with a yield that is comparable to that of the $C(^3P) + O(^3P)$ ground channel, while the J(4sσ) $^1\Sigma^+(v' = 1)$ state only dissociates through the ground channel. By integrating the areas underneath the peaks in the TKER spectra, we obtain the relative yields into different dissociation channels and thus the branching ratios. The C atoms produced in the ^3P and ^1D states are photoionized through a direct ionization process by using the photons from the same VUV beam that is used for dissociation of CO. The relative yields deduced from the TKER spectra have to be corrected for the different photoionization cross-sections of $C(^3P)$ and $C(^1D)$. A photoionization cross-section of 16 Megabarn (Mb) for $C(^3P)$ was measured by Cantu et al.[20] in the energy region of the current measurements, and the photoionization cross-section of 29 MB for $C(^1D)$ was calculated by Burke et al.[21] The uncertainties shown in Table 1 were determined by the standard deviations of three independent measurements on different days; the real uncertainties should also be affected by the accuracies of the photoionization cross-sections of $C(^3P)$ and $C(^1D)$ reported in refs 20 and 21. Using this method, we have measured the branching ratios for the nine CO states identified in the present study and listed them in Table 1.

A. W(3sσ) $^1\Pi(v' = 0, 1, 2)$. The W state is the lowest Rydberg level that converges to the first excited $CO^+(A^2\Pi)$ ion state. The vibrational progression up to $v' = 3$ has been extensively studied using the photoabsorption[22,6,23] and photoionization[7,8,24] methods to measure the rotational line widths. In the photoionization studies, the $v' = 1$ and 3 levels were not observed due to the relatively large predissociation rates of these levels. In our VUV photofragment spectra, we observed all the vibrational states with $v' = 0-3$ (the $v' = 3$ level has been reported in our previous study[15]) with the $v' = 1$ and $v' = 3$ states being greatly broadened due to the fast predissociation process, which is consistent with the previous studies. By looking into the branching ratio data for the W(3sσ) $^1\Pi(v' = 0, 1,$ and $2)$ states shown in Table 1 of the current study and the W(3sσ) $^1\Pi(v' = 3)$ state reported in our previous communication,[15] no obvious rotation and e/f-symmetry dependences of the branching ratios have been observed for the $v' = 1-3$ vibrational levels of the W(3sσ) $^1\Pi$ state, but for the $v' = 0$ leve,l a strong dependence on both the rotation and e/f-symmetry is observed for the branching ratios into the spin forbidden channel. This observation about the $v' = 0$ state is consistent with previous photoionization studies by Eikema et al.[8] and Drabbels et al.[24] In their studies, the predissociation rates of the e-symmetry levels are found to linearly depend on $J'(J' + 1)$, where J' is the rotational quantum number of the

dx.doi.org/10.1021/jp400412n | J. Phys. Chem. A XXXX, XXX, XXX−XXX

Table 1. Branching Ratios of the C(^{1}D) + O(^{3}P), C(^{3}P) + O(^{1}D), and C(^{3}P) + O(^{3}P) Product Channels for the VUV Photodissociation of CO in the Region of 102 500−106 300 cm^{-1} (12.708−13.180 eV)[a,b]

band system	VUV (cm^{-1})	rotation line (J'')	C(^{1}D) + O(^{3}P) %	C(^{3}P) + O(^{1}D) %	C(^{3}P) + O(^{3}P) %
W(3sσ) $^1\Pi(v' = 2)$	106250.5	Q(1)	1.9 ± 0.7	8.1 ± 0.3	90.0 ± 1.0
	106254.3	R(0)	2.1 ± 0.3	8.1 ± 0.4	89.8 ± 0.5
	106256.8	R(1)	1.5 ± 1.0	7.2 ± 0.5	91.3 ± 1.5
(4dσ) $^1\Sigma^+(v' = 0)$	105680.3	R(0)	0.3 ± 0.2[a]	0	99.7 ± 0.2
	105684.0	R(1)	0.4 ± 0.2	0	99.6 ± 0.2
	105687.7	R(2)	2.3 ± 0.4	0.1 ± 0.1	97.6 ± 0.5
	105691.2	R(3)	2.0 ± 0.4	0	98.0 ± 0.4
	105695.7	R(4)	9.5 ± 0.3	0.6 ± 0.1	89.9 ± 0.4
	105692.7		8.4 ± 0.5	0.6 ± 0.1	91.0 ± 0.6
	105672.7	P(1)	0.2 ± 0.1	0	99.8 ± 0.1
	105668.8	P(2)	0	0	100
L(4pπ) $^1\Pi(v' = 1)$[c]	105407.1	Q(1)			
	105411.1	R(0)	0	0	100
	105415.1	R(1)			
W(3sσ) $^1\Pi(v' = 1)$	104574.7	Q(1)	25.2 ± 0.1		74.8 ± 0.1
	104578.7	R(0)	25.6 ± 0.1		74.4 ± 0.1
	104580.9	R(1)	24.9 ± 0.3		75.1 ± 0.3
J(4sσ) $^1\Sigma^+(v' = 1)$	103687.5	P(1)	0		100
	103695.8	R(0)	0		100
	103699.0	R(1)	0		100
L(4pπ) $^1\Pi(v' = 0)$	103260.4	P(3)	6.6 ± 0.6		93.4 ± 0.6
	103264.1	P(2)	15.8 ± 0.4		84.2 ± 0.4
	103279.6	R(1)	6.3 ± 1.1		93.7 ± 1.1
	103283.8	R(2)	3.4 ± 0.4		96.6 ± 0.4
L′(3dπ) $^1\Pi(v' = 1)$	103211.2	Q(1)	51.0 ± 0.5		49.0 ± 0.5
	103215.1	R(0)	52.7 ± 0.3		47.3 ± 0.3
	103218.5	R(1)	49.2 ± 0.4		50.8 ± 0.4
	103221.7	R(2)	49.5 ± 1.0		50.5 ± 1.0
K(4pσ) $^1\Sigma^+(v' = 0)$	103027.3	P(7)	6.7 ± 0.4		93.3 ± 0.4
	103031.3	P(6)	3.8 ± 0.3		96.2 ± 0.3
	103035.3	P(5)	3.0 ± 0.4		97.0 ± 0.4
	103039.2	P(4)	2.0 ± 0.4		98.0 ± 0.4
	103043.1	P(3)	1.1 ± 0.1		98.9 ± 0.1
	103046.9	P(2)	0.4 ± 0.1		99.6 ± 0.1
	103050.8	P(1)	0		100
	103058.3	R(0)	0.5 ± 0.1		99.5 ± 0.1
	103062.2	R(1)	1.2 ± 0.1		98.8 ± 0.1
	103066.4	R(2)	2.0 ± 0.1		98.0 ± 0.1
	103069.8	R(3)	3.3 ± 0.1		96.7 ± 0.1
	103073.4	R(4)	4.8 ± 1.1		95.2 ± 1.1
	103077.3	R(5)	7.2 ± 0.5		92.8 ± 0.5
	103080.9	R(6)	6.3 ± 1.5		93.7 ± 1.5
	103084.6	R(7)	6.6 ± 0.8		93.4 ± 0.8
	103088.2	R(8)	7.9 ± 0.7		92.1 ± 0.7
	103091.6	R(9)	9.1 ± 0.5		90.9 ± 0.5
W(3sσ) $^1\Pi(v' = 0)$	102802.5	Q(3)	28.4 ± 1.5		71.6 ± 1.5
	102804.5	Q(2)	29.9 ± 0.5		70.1 ± 0.5
	102806.0	Q(1)	28.8 ± 0.4		71.2 ± 0.4
	102809.6	R(0)	19.6 ± 0.3		80.4 ± 0.3
	102812.2	R(1)	11.0 ± 0.4		89.0 ± 0.4
	102813.9	R(2)	7.1 ± 0.7		92.9 ± 0.7

[a]Photoionization cross-sections for C(^{3}P) (16 Mb) and C(^{1}D) (29 Mb) obtained from refs 20 and 21 are used in deducing the branching ratios. [b]The threshold energy for the formation of C(^{3}P) + O(^{1}D) from CO is 105 010 cm^{-1}, and thus, this channel can only be accessible for CO states at energies above this threshold energy. [c]This state is tentatively assigned as L(4pπ) $^1\Pi(v' = 1)$. It is very weak. Under the current experimental conditions, we can only see very weak signal for the ground-state product channel using the R(0) line; and no signals are detected for the two spin forbidden product channels.

upper level, while that of the f-symmetry levels are independent of the rotation angular momentum. The rotational dependence of the e-symmetry levels has been explained by the Σ to Π heterogeneous *l*-uncoupling interaction, and the repulsive $^1\Sigma^+$ state has been identified as the D′$^1\Sigma^+$ state,[25] which adiabatically correlates to the C(^{3}P) + O(^{3}P) channel. The

dx.doi.org/10.1021/jp400412n | J. Phys. Chem. A XXXX, XXX, XXX−XXX

Table 2. Comparison between the Observed Line Positions and Our Tentatively Calculated Values for the Unassigned Sequence at 105 692.50 cm^{-1} in Ref 8

J''	R(J'')[a]	obs − calcd[b]	P(J'')[a]	obs − calcd[b]	Q(J'')[a,c]	obs − calcd[b]
0	105692.50	0.00				
1	105695.81	0.01			105686.52	−2.11
2	105699.13	0.00	105682.81	1.90	105686.52	−1.56
3			105676.25	−0.24	105686.52	−1.02
4			105671.38	−0.71	105686.52	−0.85
5			105668.65	0.60	105686.52	−1.51
6			105666.02	1.17	105686.52	−3.60

[a]Experimental values obtained from Table 12 of ref 8. [b]Difference between experimental and calculated values. Calculated values are obtained by using ν_0' = 105 688.97 cm^{-1}, B' = 1.7532 cm^{-1}, and D' = −0.0049 cm^{-1}. [c]The Λ-doubling effect is not included.

predissociation of the f-symmetry levels should be caused by a $^1\Pi$ state, which is independent of J. Referring to Table 1, the branching ratio into the spin forbidden triplet channel is found to decrease with increasing J' level for the R branch; this is in accord with the fact that the predissociation rate into the ground dissociation channel increases as $J'(J'+1)$ due to the l-uncoupling interaction with the $D'^1\Sigma^+$ state. For the ν' = 2 state, Eikema et al.[8] has observed rotational dependence of the predissociation rate at high J' levels, and Eidelsberg and co-workers[6,23] also observed rotational dependence of the predissociation rate for the ν' = 2 and 3 levels, but the present results did not confirm this observation. This might be due to the relatively low detection sensitivity for this state and the fact that the populations of high J' levels are low under the supersonic molecular beam conditions. If we look at the different vibrational levels of the W state, the branching ratio also strongly depends on the vibrational quantum number. This is in accord with the fact that the W state is strongly perturbed by other Π states in this region.[4]

B. (4dσ) $^1\Sigma^+(\nu' = 0)$. The (4dσ) $^1\Sigma^+(\nu' = 0)$ state has been investigated in detail many times by photoabsorption[22,26] and photoionization[7,8] measurements, so accurate rotational constants and predissociation rates are known. We have observed this state in our C^+ ion photofragment spectrum shown in Figure 1. Eikema at al.[8] observed several local perturbations at J' = 8, 12, 19, and 22, where the peak intensities drop dramatically or even disappear from the spectrum, and the peaks around them are usually broadened due to the accidental perturbations. We have confirmed their observations in the C^+ ion photofragment spectrum for the accidental local perturbations at J' = 8, 12, and probably 19. The peaks corresponding to those rotational levels are barely seen in the C^+ ion photofragment spectrum, and the rotational levels from J' = 7 to J' = 11 are very broad. Besides those accidental perturbations, a sequence of unassigned peaks has been observed to be overlapped with the (4dσ) $^1\Sigma^+(\nu' = 0)$ state.[8] We have also observed a peak due to the unassigned sequence at 105 692.7 cm^{-1}, which is denoted by a star in Figure 1. Eikema et al. did not assign these rotational levels, nor did they report on the symmetry of the likely upper state. We have taken the time-slice VMI-PI image on the peak, and the recoil anisotropy parameter has been determined to be −0.70 ± 0.03, which indicates a strong perpendicular transition. This suggests that the peak at 105 692.7 cm^{-1} is a R(0) line belonging to a $^1\Pi$ state. On the basis of the peak positions measured by Eikema et al. shown in Table 12 of ref 8 and the current tentative assignment of the peak at 105 692.7 cm^{-1}, we guess that it is due to a $^1\Pi$ state with ν_0' = 105 688.97 cm^{-1}, B' = 1.7532 cm^{-1}, and D' = −0.0049 cm^{-1}, where ν_0', B', and D' are, respectively, the band origin, rotational constant, and centrifugal distortion constant of the upper state. Table 2 compares the line positions calculated using these constants with the experimental values reported in ref 8. The experimental and calculated values of the line positions in the R branch are in reasonable agreement with each other, but in the P and Q branches, they are not. The consistency obtained here between the branches is poor, and the centrifugal distortion is unusually large, possibly because this state is strongly perturbed. The branching ratio into the spin forbidden channels for the (4dσ) $^1\Sigma^+(\nu' = 0)$ state listed in Table 1 shows an unusual rotational dependence, which may be due to the overlapped unassigned band.

C. L(4pπ) $^1\Pi(\nu' = 0, 1)$. The L(4pπ) $^1\Pi(\nu' = 0)$ state has been a model system for studying the predissociation dynamics of CO and thus has been investigated many times with various experimental methods.[22,7−11,24,27,28] The predissociation rates of the e-symmetry levels were found to linearly increase with $J'(J'+1)$, which is explained by the interaction with the repulsive $D'^1\Sigma^+$ state. Besides the rotational dependent part, the predissociation rates of the e-symmetry levels also contain a rotation independent part (k_0), and the f-symmetry levels are also strongly predissociative. The latter predissociation could be caused by a homogeneous interaction with a repulsive $^1\Pi$ state. The photofragment spectra of Okazaki et al.[10,11] that probed both $C(^3P)$ and $C(^1D)$ showed that CO molecules in the L(4pπ) $^1\Pi(\nu' = 0)$ state not only dissociate to the channel producing ground state atoms but also to the triplet channel that produces $C(^1D)$ and $O(^3P)$. They also showed that the branching ratio between these two channels depends on both the rotational quantum number and the e/f-symmetry. We have reinvestigated this state by using the VUV time-slice VMI-PI imaging method. The C^+ ion photofragment spectrum is shown in Figure 2, and the branching ratio measurement is listed in Table 1. Because of the very strong CO^+ ion intensity produced in the interaction region,[8] the space charge effect prevents us from taking good images for the R(0) and Q(1) lines. A similar phenomenon to the W(3sσ) $^1\Pi(\nu' = 0)$ state has been observed, the branching ratio into the triplet channel decreases as J' increases. This is consistent with the fact that the predissociation rate into the ground channel caused by the $D'^1\Sigma^+$ state is increasing with $J'(J'+1)$. The R(1) line and P(3) line have the same branching ratio within the experimental uncertainty because they share the same upper level with J' = 2 in the L(4pπ) $^1\Pi(\nu' = 0)$ state.

Compared with the ν' = 0 level discussed above, the first excited ν' = 1 vibrational level of the L(4pπ) $^1\Pi$ state has been rarely studied mainly due to its very weak absorption cross-section from the vibronic ground state of CO. It was observed in the absorption spectrum by Eidelsberg and co-workers[22,29] at

dx.doi.org/10.1021/jp400412n | J. Phys. Chem. A XXXX, XXX, XXX−XXX

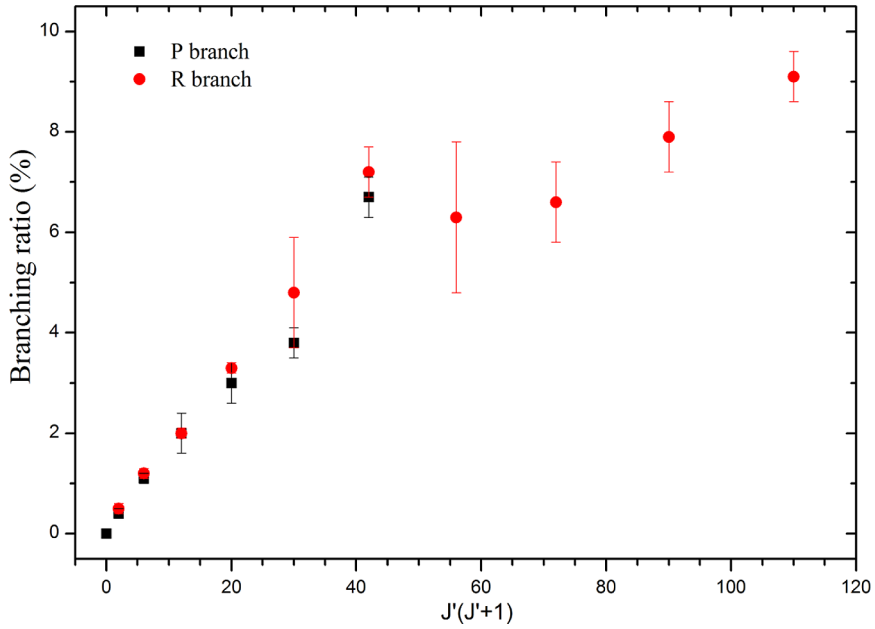

Figure 5. Dependence of the branching ratio for the dissociation of the K(4pσ) $^1\Sigma^+(v' = 0)$ state into the spin forbidden product channel, C(^{1}D) +O(^{3}P), on $J'(J' + 1)$. J' is the rotational quantum number of the upper level. The black squares and red dots correspond to the measurements of P and R branches, respectively.

around 105 442 cm^{-1} and calculated by Lefebvre-Brion et al.[30] to be at 105 379 cm^{-1}. We have employed the newly built VUV-VUV pump−probe time-slice VMI imaging setup[31] to study CO in this region. The probing VUV was fixed at 78 293.07 cm^{-1} to be resonant with the transition C(^{3}P$_0$) → 2s^{2}2p3d (^{3}D$_1$); the excited carbon atoms in this 2s^{2}2p3d (^{3}D$_1$) state are ionized by absorbing a second UV photon (ω_1) accompanying the VUV beam. We scanned the pump VUV and got the C$^+$ ion photofragment spectrum for the L(4pπ) $^1\Pi(v' = 1)$ state as shown in Figure 1. The use of a second VUV laser for (1 + 1′) REMPI ionization greatly increases the detection sensitivity, which allows us to detect such a weak absorption band. The tentative rotational assignment is shown in Figure 1 by drop lines. The band origin and rotational constant were determined to be 105 407.1 cm^{-1} and 1.983 cm^{-1}, which are compared with the respective experimental values of 105 442 cm^{-1} and 1.9606 cm^{-1} obtained by Eidelsberg and co-workers[22,29] and the theoretical values of 105 379 cm^{-1} and 1.906 cm^{-1} calculated by Lefebvre-Brion at al.[30] From the spectrum shown in Figure 1, it is obvious that the rotational lines are broadened with increasing J' levels in the R branch. This is due to the interaction with the D′$^1\Sigma^+$ state. A broadened Q(1) line with a line width even larger than that of the R(0) line was also observed. This implies that there is a perturbation between this state and a $^1\Pi$ state that is causing a fast predissociation rate for the f-symmetry levels. A similar effect is also observed in the L(4pπ) $^1\Pi(v' = 0)$ state.[9] No signal is observed into the triplet channel that produces C(^{1}D)+O(^{3}P) for the L(4pπ) $^1\Pi(v' = 1)$ state as shown in Table 1.

D. L′(3dπ) $^1\Pi$ ($v' = 1$). The L′(3dπ) $^1\Pi$ ($v' = 1$) state is very close to the L(4pπ) $^1\Pi(v' = 0)$ state, and the strong coupling between these two $^1\Pi$ states has been analyzed before.[27,28] This state was found to be strongly predissociative[22,7] and only a very weak signal was observed in the photoionization spectrum.[8,24] The predissociation rate is independent of both the rotation and e/f-symmetry.[8,11,24] Okazaki et al.[10,11] have obtained the C$^+$ ion photofragment spectrum by probing both C(^{3}P) and C(^{1}D) and concluded that the predissociation rates to the ground channel and the triplet channel producing C(^{1}D) are comparable to each other and that the ratio between them is independent of the rotation and e/f-symmetry. We have observed a very strong signal in our C$^+$ ion photofragment spectrum for this state, as shown in Figure 2. The branching ratio data are given in Table 1. The percentage into the spin forbidden channel is almost the same as it is into the spin allowed channel, and the ratio between them does not depend on the rotation or e/f-symmetry of the level within the experimental uncertainty. All of this is in good agreement with the conclusion by Okazaki et al.[10,11]

E. K(4pσ) $^1\Sigma^+$ ($v' = 0$). The predissociation rates of this state have been measured by Drabbels et al.[24] at low J' levels and found to be independent of the rotational quantum number. It was confirmed by Eikema et al.[8] at high J' levels up to 20. It implies that the predissociation of the K(4pσ) $^1\Sigma^+(v' = 0)$ state is caused by the homogeneous $^1\Sigma^+-^1\Sigma^+$ interaction. Okazaki et al.[10,11] did not see any signal in the C(^{1}D) photofragment spectrum for this state. We have reinvestigated this state by using our VUV time-slice VMI-PI imaging method. The C$^+$ ion photofragment spectrum shown in Figure 2 is completely regular just as the photoionization spectrum obtained by Eikema et al.,[8] and the branching ratio data listed in Table 1 shows that there is a small percentage of CO dissociating into the spin forbidden channel that was not observed by Okazaki et al.[10,11] The branching ratio of the spin forbidden channel increases as the rotational quantum number increases. We have plotted the ratio versus $J'(J' + 1)$ as shown in Figure 5. From this figure, we can see that the percentage into the spin forbidden channel is nearly linearly dependent on $J'(J' + 1)$. The branching ratios obtained for a particular J' from the P and R branches are consistent with each other within the experimental uncertainty. This observation was not made by the previous experiments that focused on measuring the rotational line widths.[8,24] A local perturbation may exist at the upper $J' = 6$ level that causes the branching ratio to be a little

dx.doi.org/10.1021/jp400412n | J. Phys. Chem. A XXXX, XXX, XXX−XXX

higher than the trend. A linear dependence of the percentage of the triplet channel on $J'(J'+1)$ implies that there is an interaction with a $^1\Pi$ state that occurs in the process of dissociation into the triplet channel $C(^1D) + O(^3P)$.

F. J(4sσ) $^1\Sigma^+$ (v' = 1). The $J(4s\sigma)\ ^1\Sigma^+$ (v' = 1) state has been observed to be strongly dissociative with a lifetime in the order of picoseconds,[22,32] and thus, it has not been observed in any of the photoionization spectra. It was only identified in the absorption spectrum of CO by Eidelsberg et al.[22] and in the ion-dip spectrum by Komatsu et al.[32] The band origins and rotational constants obtained by the two different methods are consistent with each other. We have obtained a C^+ ion photofragment spectrum for this state and show it in Figure 3. The drop lines show the rotational levels calculated using the band origin and rotational constant by Eidelsberg et al.[22] No individual rotational lines can be resolved in the spectrum, which is consistent with the fact that it is strongly dissociative. The branching ratio of the spin-forbidden channel is zero as shown in Table 1, thus it does not dissociate into the triplet channel $C(^1D) + O(^3P)$. Komatsu et al.[32] tried to understand the predissociation dynamics for this state into the ground channel; they tentatively concluded that it is more likely this state is interacting with a repulsive $^1\Pi$ state other than the well-known $D'^1\Sigma^+$ state. With the information in the present study, we cannot determine the repulsive state that is responsible for the dissociation of the $J(4s\sigma)\ ^1\Sigma^+(v'=1)$ state into the channel of $C(^3P) + O(^3P)$.

IV. DISCUSSION

Previous experiments based on the measurements of rotational line widths[7,8,24] or the time-delay pump−probe lifetime measurements[9] cannot distinguish between the spin allowed and forbidden channels. Thus, they cannot study the predissociation dynamics with the kind of detail described in this article. Since the spin-allowed $[C(^3P) + O(^3P)]$ and the spin-forbidden $[C(^1D) + O(^3P)]$ channels correlate with the singlet and triplet potential energy surfaces, we refer to these channels below as the singlet and triplet channels, respectively. With the present tunable VUV laser time-slice VMI-PI method, we have been able to distinguish the spin-allowed and spin-forbidden channels and to measure their branching ratios. This should shed light on the predissociation dynamics of CO, particularly the aspect involving the formation of the spin forbidden triplet channels. The fractions of the triplet and singlet channels can be expressed as follows:

$$P_T = k_T/(k_T + k_S) \quad (1)$$

$$P_S = k_S/(k_T + k_S) \quad (2)$$

where k_T and k_S are the corresponding predissociation rate constants into the triplet and singlet channels, respectively. The branching ratio between them will be

$$R = P_T/P_S = k_T/k_S \quad (3)$$

If the *l*-uncoupling perturbation is occurring in the predissociation process, a dependence of the predissociation rate constant on the rotational quantum number should be observed. For a $^1\Pi-^1\Sigma^+$ heterogeneous interaction, the predissociation rate constant is expected to be linearly dependent on $J'(J'+1)$, where J' is the rotational quantum number of the excited vibronic state.[33,34] If this happens in the predissociation process into the triplet channels, then the branching ratio can be rewritten as

$$R = [k_0^T + k_J^T J'(J'+1)]/k_S \quad (4)$$

then

$$R = k_0^T/k_S + (k_J^T/k_S)J'(J'+1) \quad (5)$$

Similarly, if the heterogeneous interaction happens in the predissociation process into the ground singlet channel, then the ratio can be rewritten as

$$1/R = [k_0^S + k_J^S J'(J'+1)]/k_T \quad (6)$$

then

$$1/R = k_0^S/k_T + (k_J^S/k_T)J'(J'+1) \quad (7)$$

Here, k_0^T and k_0^S (k_J^T and k_J^S) are the rotational independent (rotational dependent) part of the predissociation rate constants for the triplet and singlet channels, respectively. On the basis of eqs 5 and 7, the ratio R or $1/R$ will linearly depend on $J'(J'+1)$ if a $^1\Pi-^1\Sigma^+$ heterogeneous interaction occurs during the predissociation process.

We plot the $1/R$ value versus $J'(J'+1)$ in Figure 6 for the CO states $L(4p\pi)\ ^1\Pi(v'=0)$ and $W(3s\sigma)\ ^1\Pi(v'=0)$, and the

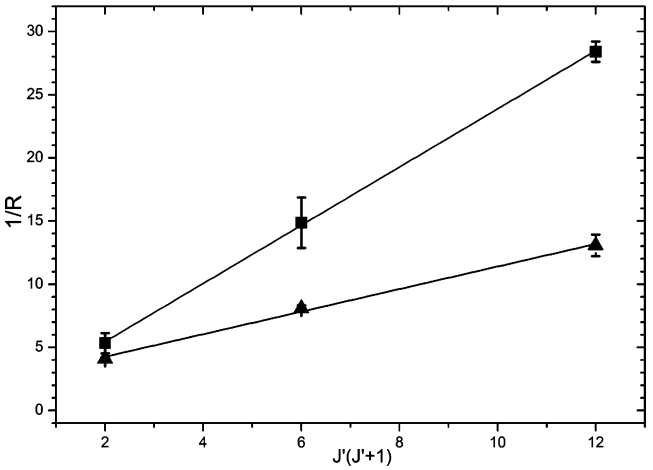

Figure 6. Dependence of the ratio $1/R$ (see the text) on $J'(J'+1)$;, J' is the rotational quantum number of the upper level. The black squares and triangles correspond to the experimental measurements of the $L(4p\pi)\ ^1\Pi(v'=0)$ and $W(3s\sigma)\ ^1\Pi(v'=0)$ states, respectively. The straight lines are the linear fittings.

linear fittings according to eq 7 are also shown by lines in the figure. A good match between the linear fittings and the experimental measurements is observed for both of the $^1\Pi$ states of CO. According to the above discussion of eq 7, the dissociation into the singlet channel should involve a $^1\Pi-^1\Sigma^+$ heterogeneous interaction. At the same time, the intercepts of the two lines are nonzero values, which mean that the rotational independent part k_0^S of the two states are not zero. This observation is in agreement with previous studies[8,11,24] that both $^1\Pi-^1\Sigma^+$ and $^1\Pi-^1\Pi$ interactions play important roles in the predissociation of CO into the singlet channel and that the repulsive $^1\Sigma^+$ state has been identified as the $D'^1\Sigma^+$ state, but the $^1\Pi$ state has not yet been identified.[2,17] According to the perfect linear dependence of the $1/R$ value on $J'(J'+1)$, we should also be able to conclude that k_T in eq 7 does not depend on the rotational quantum number J'. This explains why Okazaki et al.[11] can use k_0^T, which is equivalent to k_T here, as a parameter (independent of the rotational quantum number J')

dx.doi.org/10.1021/jp400412n | J. Phys. Chem. A XXXX, XXX, XXX−XXX

to simulate their photofragment yield spectra. For the K(4pσ) $^1\Sigma^+(v' = 0)$ state, the percentage into the triplet channel is much smaller than that into the singlet channel; thus, the ratio $R = k_T/k_S \approx k_T/(k_T + k_S) = P_T$. How the fraction of the triplet channel P_T and thus the ratio R depends on the rotational quantum number J' has been shown in Figure 5. A linear dependence is clear with an intercept of zero, which means k_0^T is equal to zero; thus, the predissociation of the K(4pσ) $^1\Sigma^+(v' = 0)$ state into the triplet channel is a purely l-uncoupling induced result. Because of the fact that the rotational line width is independent of the rotational quantum number J',[8] the predissociation of the K(4pσ) $^1\Sigma^+(v' = 0)$ state into the ground state channel should be mainly caused by the homogeneous interaction with the D′$^1\Sigma^+$ state instead of $^1\Pi$ valence states.

Only the triplet valence states can correlate to the channel of C(^{1}D) + O(^{3}P) according to O′Neil and Schaefer's theoretical calculation.[35] By looking at the potential energy curves of those triplet states predicted by O′Neil and Schaefer,[35] we find that only the $3^3\Pi$ and $2^3\Sigma^-$ states cross with those excited Rydberg states in the Franck−Condon region. The first order perturbation between a $^3\Sigma^-$ state and a $^1\Sigma^+$ state is independent of J';[33] the perturbation between a $^3\Sigma^-$ state and a $^1\Pi$ state is nonlinearly dependent on J'.[33] Neither of the above two phenomena has been observed; thus, it is more likely that the $3^3\Pi$ valence state is playing an important role in the predissociation process into the triplet channel. Direct coupling between a $^3\Pi$ state and $^1\Sigma^+$ does not depend on J′ in Hund case (a) and not linearly on $J'(J' + 1)$ in case (b);[33] there have to be certain intermediate states that connect the directly excited Rydberg state and the final repulsive $3^3\Pi$ state. The l-uncoupling interaction between a $^1\Sigma^+$ state and a $^1\Pi$ state is linearly dependent on $J'(J' + 1)$,[33,34] and the spin−orbit coupling between a $^1\Pi$ state and a $^3\Pi$ state is independent of the rotational quantum number J'.[33] On the basis of the discussion thus far, we propose a predissociation mechanism that has a coupling scheme of $^1\Sigma^+-^1\Pi-^3\Pi$ for the predissociation of the K(4pσ) $^1\Sigma^+(v' = 0)$ state into the triplet channel. The directly excited $^1\Sigma^+$ state first couples to an intermediate $^1\Pi$ state, that coupling linearly depends on $J'(J' + 1)$; the intermediate $^1\Pi$ state then couples to the repulsive $^3\Pi$ state through a spin−orbit interaction, which does not depend on J'. This mechanism can explain the linear dependence of the triplet channel on $J'(J' + 1)$ for the K(4pσ) $^1\Sigma^+(v' = 0)$ state shown in Figure 5. If it is a $^1\Pi$ Rydberg state being excited, a coupling scheme of $^1\Pi-^1\Pi-^3\Pi$ (or simply $^1\Pi-^3\Pi$) will result in rotationally independent predissociation into the triplet channel, this has been directly observed for the W(3sσ) $^1\Pi(v' = 1, 2)$ and L′(3dπ) $^1\Pi(v' = 1)$ states as shown in Table 1; for the L(4pπ) $^1\Pi(v' = 0)$ and W(3sσ) $^1\Pi(v' = 0)$ states, a rotationally independent predissociation into the triplet channel has also been confirmed based on the above discussion. So a predissociation mechanism involving a $^1\Pi$ intermediate state and a $^3\Pi$ final repulsive state correlating to the triplet channel can generally explain the branching ratio data into the spin-forbidden channel in the present work. It is in agreement with our previous tentatively proposed predissociation mechanism for the spin-forbidden channels.[16] The same predissociation mechanism has also been confirmed for N_2, which is isoelectronic with CO.[36,37] Compared with the L(4pπ) $^1\Pi(v' = 0)$ and W(3sσ) $^1\Pi(v' = 0)$ states, no rotational and e/f-symmetry dependence of the branching ratio into the triplet channel can be deduced for the W(3sσ) $^1\Pi(v' = 1, 2)$ and L′(3dπ) $^1\Pi$ $(v' = 1)$ states implying that they are not coupling with the D′$^1\Sigma^+$ state according to eq 7, and thus, a different predissociation mechanism involving a $^1\Pi$ valence state is probably responsible for the W(3sσ) $^1\Pi(v' = 1, 2)$ and L′(3dπ) $^1\Pi(v' = 1)$ states to dissociate into the ground state channel. The L(4pπ) $^1\Pi(v' = 1)$ and J(4sσ) $^1\Sigma^+(v' = 1)$ states do not dissociate into the triplet channel; thus, they are not coupling to the intermediate $^1\Pi$ state that interacts with the repulsive $^3\Pi$ state correlating to the triplet channel. For the L(4pπ) $^1\Pi(v' = 1)$ state, the rotational line width in the R branch increases as increasing J', and the Q branch also dissociates; thus, both the D′$^1\Sigma^+$ and the unidentified $^1\Pi$ valence state interact with the L(4pπ) $^1\Pi(v' = 1)$ state. For the J(4sσ) $^1\Sigma^+(v' = 1)$ state, it is not sure what kind of repulsive state is responsible for the predissociation to the ground state channel.

According to the discussion so far, three different pathways have been identified for CO to dissociate into the atomic products: (I) the excited Rydberg states couple to the D′$^1\Sigma^+$ valence state to produce C(^{3}P) + O(^{3}P); (II) the excited Rydberg states couple to $^1\Pi$ valence states to produce C(^{3}P) + O(^{3}P); (III) the excited Rydberg states couple to an intermediate $^1\Pi$ state (Rydberg or valence), then the intermediate $^1\Pi$ state couples to a $^3\Pi$ valence state to produce C(^{1}D) + O(^{3}P). We have summarized in Table 3 how each of the three predissociation pathways are applied to the nine CO vibronic states investigated in the present study. For the (4dσ) $^1\Sigma^+(v' = 0)$ state, there are many accidental perturbations, which should be caused by interactions with certain bound states.[8] The predissociation into the spin-forbidden channel seems to be caused through borrowing intensity from the unassigned $^1\Pi$ state. All of these make it difficult to deduce the possible predissociation dynamics. Thus, we indicate in Table 3 that the detailed predissociation mechansim for the (4dσ) $^1\Sigma^+(v' = 0)$ state is still uncertain.

Table 3. Summary of How Each of the Three Predissociation Pathways Applies to the Nine CO Vibronic States Investigated in the Present Study[a,b]

vibronic states of CO	pathway (I)	pathway (II)	pathway (III)
W(3sσ) $^1\Pi(v' = 2)$	N	Y	Y
(4dσ) $^1\Sigma^+(v' = 0)$	c	c	c
L(4pπ) $^1\Pi(v' = 1)$	Y	Y	N
W(3sσ) $^1\Pi(v' = 1)$	N	Y	Y
J(4sσ) $^1\Sigma^+(v' = 1)$	c	c	N
L(4pπ) $^1\Pi(v' = 0)$	Y	Y	Y
L′(3dπ) $^1\Pi(v' = 1)$	N	Y	Y
K(4pσ) $^1\Sigma^+(v' = 0)$	Y	N	Y
W(3sσ) $^1\Pi(v' = 0)$	Y	Y	Y

[a]For the definitions of pathway (I), (II), and (III), please refer to the text. [b]Y and N indicate the pathways are applicable and not applicable, respectively, to the predissociation of CO excited to the vibronic states. [c]Mechanism uncertain. See the text.

V. SUMMARY AND CONCLUSIONS

In summary, the branching ratios for the production of the spin-forbidden product channels by predissociation of CO in the energy region from 102 500 (12.708 eV) to 106 300 cm^{-1} (13.180 eV) were measured. Rotation and e/f-symmetry dependences of the branching ratios have been observed for several of the dissociation states in this region, and it has been explained by a R−$^1\Pi-^3\Pi$ coupling scheme, where R represents the initially excited Rydberg state. To identify the intermediate

dx.doi.org/10.1021/jp400412n | J. Phys. Chem. A XXXX, XXX, XXX−XXX

$^1\Pi$ state and the final repulsive $^3\Pi$ state, detailed ab initio calculations are needed. Theoretical calculation of the potential energy curves of CO has been reported by Lefebvre-Brion and co-workers,[4] where the singlet and triplet Π potential energy curves in the valence region are predicted, which are important to the understanding of the predissociation dynamics of CO. The possible $^1\Pi-^1\Pi$ and $^3\Pi-^3\Pi$ interactions have been included in their calculation. However, the spin−orbit interaction between the $^1\Pi$ and $^3\Pi$ states, which has been shown to be important in the predissociation of CO by the present study, has not been investigated in detail. For predissociation into the spin allowed channel that produces ground state atoms, this study shows that additional valence $^1\Pi$ states have to be involved and play a role beside that of the well-known $D'^1\Sigma^+$ state. It may be that this unknown perturber is the $E'^1\Pi$ state as suggested by Lefebvre-Brion et al.[17,4,38] To understand the detailed predissociation dynamics, further theoretical calculations are strongly needed. We hope that the present experimental study would serve to provide a benchmark and stimulate more extensive and accurate theoretical calculations in the future for a more detailed understanding of the CO photodissociation dynamics.

AUTHOR INFORMATION

Corresponding Author

*(W.M.J.) E-mail: wmjackson@ucdavis.edu. Phone: 530-742-0504. (C.Y.N.) E-mail: cyng@ucdavis.edu. Phone: 530-754-9645.

Notes

The authors declare no competing financial interest.

ACKNOWLEDGMENTS

H.G., Y.S., and W.M.J. were supported by National Science Foundation under grant # CHE-0957872. H.G., Y.-C.C., and C.Y.N. were supported by U.S. Department of Energy on Contract # DEFG02-02ER15306. Y.-C.C., Q.-Z.Y., C.Y.N., and R.C.W. acknowledge the support of a LANL-UC IGPP grant. We are also grateful to Prof. H. Lefebvre-Brion for helpful discussions.

REFERENCES

(1) Clayton, R. N. Solar System: Self-Shielding in the Solar Nebula. *Nature* **2002**, *415*, 860.

(2) Visser, R.; van Dishoeck, E. F.; Black, J. H. The Photodissociation and Chemistry of CO Isotopologues: Applications to Interstellar Clouds and Circumstellar Disks. *Astron. Astrophys.* **2009**, *503*, 323.

(3) Huber, K. P. Solved and Unsolved Problems of Near-Threshold Spectroscopy of N_2 and CO. *Philos. Trans. R. Soc. London Ser. A* **1997**, *355*, 1527.

(4) Vázquez, G. J.; Amero, J. M.; Liebermann, H. P.; Lefebvre-Brion, H. Potential Energy Curves for the $^1\Sigma^+$ and $^{1,3}\Pi$ States of CO. *J. Phys. Chem. A* **2009**, *113*, 13395.

(5) Letzelter, C.; Eidelsberg, M.; Rostas, F.; Breton, J.; Thieblemont, B. Photoabsorption and Photodissociation Cross-Sections of CO Between 88.5 and 115 nm. *Chem. Phys.* **1987**, *114*, 273.

(6) Eidelsberg, M.; Lemaire, J. L.; Federman, S. R.; Stark, G.; Heays, A. N.; Sheffer, Y.; Gavilan, L.; Fillion, J.-H.; Rostas, F.; Lyons, J. R.; et al. High-Resolution Study of Oscillator Strengths and Predissociation Rates for $^{12}C^{16}O$. *Astron. Astrophys.* **2012**, *543*, A69.

(7) Levelt, P. F.; Ubachs, W.; Hogervorst, W. Extreme Ultraviolet-Laser Spectroscopy on CO in the 91−100 nm Range. *J. Chem. Phys.* **1992**, *97*, 7160.

(8) Eikema, K. S. E.; Hogervorst, W.; Ubachs, W. Predissociation Rates in Carbon-Monoxide: Dependence on Rotational State, Parity and Isotope. *Chem. Phys.* **1994**, *181*, 217.

(9) Cacciani, P.; Brandi, F.; Sprengers, J. P.; Johansson, A.; L'Huillier, A.; Wahlström, C. G.; Ubachs, W. Predissociation of the 4pπ $L^1\Pi$ Rydberg State of Carbon Monoxide. *Chem. Phys.* **2002**, *282*, 63.

(10) Okazaki, A.; Ebata, T.; Sutani, T.; Mikami, N. Predissociation of the Rydberg States of CO: State Specific Predissociation to the Triplet Channel. *J. Chem. Phys.* **1998**, *108*, 1765.

(11) Okazaki, A.; Ebata, T.; Mikami, N. Predissociation of Rydberg States of CO Investigated by the Detection of Atomic Fragments. *J. Chem. Phys.* **2001**, *114*, 7886.

(12) Bakker, B. L. G.; Parker, D. H. Photodissociation Dynamics of $^{13}C^{16}O$ Excited by 193 nm Light. *Chem. Phys. Lett.* **2000**, *330*, 293.

(13) Pan, Y.; Gao, H.; Yang, L.; Zhou, J.; Ng, C. Y.; Jackson, W. M. Vacuum Ultraviolet Laser Photodissociation Studies of Small Molecules by the Vacuum Ultraviolet Laser Photoionization Time-Sliced Velocity-Mapped Ion Imaging Method. *J. Chem. Phys.* **2011**, *135*, 071101.

(14) Gao, H.; Pan, Y.; Yang, L.; Zhou, J.; Ng, C. Y.; Jackson, W. M. Time-Slice Velocity-Map Ion Imaging Studies of the Photodissociation of NO in the Vacuum Ultraviolet Region. *J. Chem. Phys.* **2012**, *136*, 134302.

(15) Gao, H.; Song, Y.; Yang, L.; Shi, X.; Yin, Q.; Ng, C. Y.; Jackson, W. M. Branching Ratio Measurements in the Predissociation of $^{12}C^{16}O$ by Time-Slice Velocity-Map Ion Imaging in the Vacuum Ultraviolet Region. *J. Chem. Phys.* **2011**, *135*, 221101.

(16) Gao, H.; Song, Y.; Yang, L.; Shi, X.; Yin, Q.-Z.; Ng, C. Y.; Jackson, W. M. Branching Ratio Measurements of the Predissociation of $^{12}C^{16}O$ by Time-Slice Velocity-Map Ion Imaging in the Energy Region From 108 000 to 110 500 cm^{-1}. *J. Chem. Phys.* **2012**, *137*, 034305.

(17) Lefebvre-Brion, H.; Lewis, B. R. Comparison Between Predissociation Mechanisms in Two Isoelectronic Molecules: CO and N_2. *Mol. Phys.* **2007**, *105*, 1625.

(18) Zhou, J.; Lau, K.-C.; Hassanein, E.; Xu, H.; Tian, S.-X.; Jones, B.; Ng, C. Y. A Photodissociation Study of CH_2BrCl in the *A*-Band Using the Time-Sliced Ion Velocity Imaging Method. *J. Chem. Phys.* **2006**, *124*, 034309.

(19) Jones, B.; Zhou, J.; Yang, L.; Ng, C. Y. High-Resolution Rydberg Tagging Time-of-Flight Measurements of Atomic Photofragments by Single-Photon Vacuum Ultraviolet Laser Excitation. *Rev. Sci. Instrum.* **2008**, *79*, 123106.

(20) Cantu, A. W.; Mazzoni, M.; Pettini, M.; Tozzi, G. P. Photoionization Spectrum of the ^3P Ground State of Neutral Carbon. *Phys. Rev. A* **1981**, *23*, 1223.

(21) Burke, P. G.; Taylor, K. T. Photoionization of Carbon Atoms. *J. Phys. B: At., Mol. Opt. Phys.* **1979**, *12*, 2971.

(22) Eidelsberg, M.; Rostas, F. Spectroscopic, Absorption and Photodissociation Data for CO and Isotopic-Species Between 91 and 115 nm. *Astron. Astrophys.* **1990**, *235*, 472.

(23) Eidelsberg, M.; Sheffer, Y.; Federman, S. R.; Lemaire, J. L.; Fillion, J. H.; Rostas, F.; Ruiz, J. Oscillator Strengths and Predissociation Rates for Rydberg Transitions in $^{12}C^{16}O$, $^{13}C^{16}O$, and $^{13}C^{18}O$ Involving the E $^1\Pi$, B $^1\Sigma^+$ and W $^1\Pi$ States. *Astrophys. J.* **2006**, *647*, 1543.

(24) Drabbels, M.; Heinze, J.; Termeulen, J. J.; Meerts, W. L. High-Resolution Double-Resonance Spectroscopy on Rydberg States of CO. *J. Chem. Phys.* **1993**, *99*, 5701.

(25) Wolk, G. L.; Rich, J. W. Observation of a New Electronic State of Carbon Monoxide Using LIF on Highly Vibrationally Excited $CO(X^1\Sigma^+)$. *J. Chem. Phys.* **1983**, *79*, 12.

(26) Ubachs, W.; Eikema, K. S. E.; Levelt, P. F.; Hogervorst, W.; Drabbels, M.; Meerts, W. L.; Meulen, J. J. T. Accurate Determination of Predissociation Rates and Transition Frequencies for Carbon Monoxide. *Astrophys. J.* **1994**, *427*, L55.

(27) Eidelsberg, M.; Launay, F.; Ito, K.; Matsui, T.; Hinnen, P. C.; Reinhold, E.; Ubachs, W.; Huber, K. P. Rydberg−Valence Interactions

of CO, and Spectroscopic Evidence Characterizing the C $^1\Sigma^+$ Valence State. *J. Chem. Phys.* **2004**, *121*, 292.
(28) Rostas, F.; Launay, F.; Eidelsberg, M.; Benharrous, M.; Blaess, C.; Huber, K. P. Extreme UV Absorption-Spectroscopy of CO Isotopomers in Pulsed Supersonic Free Jet Expansions. *Can. J. Phys.* **1994**, *72*, 913.
(29) Eidelsberg, M.; Benayoun, J. J.; Viala, Y.; Rostas, F.; Smith, P. L.; Yoshino, K.; Stark, G.; Shettle, C. A. Recalibration of the Absorption/Photodissociation Spectra of CO and Its Isotopes Between 91 and 115 nm. *Astron. Astrophys.* **1992**, *265*, 839.
(30) Lefebvre-Brion, H.; Eidelsberg, M. New Experimental Study and Theoretical Model of the Extreme UV Absorption Spectrum of CO Isotopologs. *J. Mol. Spectrosc.* **2012**, *271*, 59.
(31) Song, Y.; Gao, H.; Ng, C. Y.; Jackson, W. M. Combining Two VUV Lasers with the Time-Sliced Velocity Mapped Ion Imaging Method for Studying the Photodissociation of Small Molecules. *EAS Publ. Ser.* **2012**, *58*, 295−299.
(32) Komatsu, M.; Ebata, T.; Maeyama, T.; Mikami, N. Rotational Structure and Dissociation of the Rydberg States of CO Investigated by Ion-Dip Spectroscopy. *J. Chem. Phys.* **1995**, *103*, 2420.
(33) Kovacs, I. *Rotational Structure in the Spectra of Diatomic Molecules*; Adam Hilger: London, 1969.
(34) Lefebvre-Brion, H.; Field, R. W. *The Spectra and Dynamics of Diatomic Molecules*; Elsevier: New York, 2004.
(35) O'Neil, S. V.; Schaefer, H. F., III. Valence-Excited States of Carbon Monoxide. *J. Chem. Phys.* **1970**, *53*, 3994.
(36) Buijsse, B.; van der Zande, W. J. The Predissociation Mechanisms of the e $^1\Pi_u$ and the b′ $^1\Sigma_u^+$ States of N_2. *J. Chem. Phys.* **1997**, *107*, 9447.
(37) Lewis, B. R.; Gibson, S. T.; Zhang, W.; Lefebvre-Brion, H.; Robbe, J. M. Predissociation Mechanism for the Lowest $^1\Pi_\mu$ States of N_2. *J. Chem. Phys.* **2005**, *122*, 144302.
(38) Lefebvre-Brion, H.; Liebermann, H. P.; Vazquez, G. J. An Interpretation of the Anomalous $^1\Pi$ Vibronic Structure in the Far-UV Spectrum of CO. *J. Chem. Phys.* **2010**, *132*, 024311.